Article

Electron Transfer and Catalytic Control by the Iron–Sulfur Clusters in a Respiratory Enzyme, *E. coli* Fumarate Reductase

Janette M. Hudson, Kerensa Heffron, Violetta Kotlyar, Yelizaveta Sher, Elena Maklashina, Gary Cecchini, and Fraser A. Armstrong

J. Am. Chem. Soc., **2005**, 127 (19), 6977-6989• DOI: 10.1021/ja043404q • Publication Date (Web): 22 April 2005

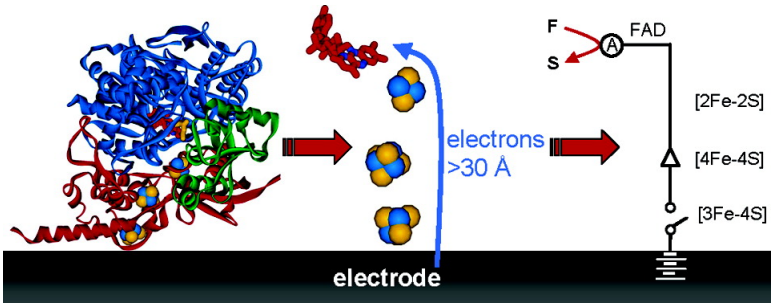

More About This Article

Additional resources and features associated with this article are available within the HTML version:

- Supporting Information
- Links to the 12 articles that cite this article, as of the time of this article download
- Access to high resolution figures
- Links to articles and content related to this article
- Copyright permission to reproduce figures and/or text from this article

View the Full Text HTML

J|A|C|S
ARTICLES
Published on Web 04/22/2005

Electron Transfer and Catalytic Control by the Iron−Sulfur Clusters in a Respiratory Enzyme, *E. coli* Fumarate Reductase

Janette M. Hudson,[†] Kerensa Heffron,[†] Violetta Kotlyar,[‡] Yelizaveta Sher,[‡] Elena Maklashina,[‡] Gary Cecchini,*[,‡] and Fraser A. Armstrong*[,†]

Contribution from the Department of Chemistry, Inorganic Chemistry Laboratory, Oxford University, South Parks Road, Oxford OX1 3QR, U.K., the Molecular Biology Division, Department of Veterans Affairs Medical Center, San Francisco, California 94121, and Department of Biochemistry and Biophysics, University of California, San Francisco, California 94143

Received November 1, 2004; E-mail: fraser.armstrong@chem.ox.ac.uk (F.A.A.); ceccini@itsa.ucsf.edu (G.C.)

Abstract: Factors governing the efficacy of long-range electron relays in enzymes have been examined using protein film voltammetry in conjunction with site-directed mutagenesis. Investigations of the fumarate reductase from *Escherichia coli*, in which three Fe−S clusters relay electrons over more than 30 Å, lead to the conclusion that varying the medial [4Fe−4S] cluster potential over a 100 mV range does not have a significant effect on the inherent kinetics of electron transfer to and from the active-site flavin. The results support a proposal that the reduction potential of an individual electron relay site in a multicentered enzyme is not a strong determinant of activity; instead, as deduced from the potential dependence of catalytic electron transfer, electron flow through the intramolecular relay is rapid and reversible, and even uphill steps do not limit the catalytic rate.

Iron−sulfur (Fe−S) clusters abound in large redox enzymes, particularly membrane-bound respiratory systems,[1−3] and it is tacitly assumed that their main role is to mediate long-range electron transfer (ET). However, the importance of the reduction potential of individual Fe−S clusters, or indeed any redox center in a relay series, has rarely been established. Examples of enzymes with a high catalytic rate despite one of the relay centers having a singularly high or low reduction potential (thus tending to trap or obstruct electrons) include [NiFe]-hydrogenases,[4] dissimilatory nitrate reductases,[5] and fumarate reductase from *Escherichia coli*.[6] It might be expected that these enzymes should perform even more efficiently (conferring an evolutionary advantage) were the ET energetics to be more uniform. However, on the basis of structural and kinetic data available for many enzymes, Dutton and co-workers have argued that the feature most strongly selected for in the evolution of protein ET relays is an intersite tunneling distance less than ∼14 Å.[7] Thus, the robustness of ET to mutations that alter reduction potentials is set forth where, as long as the cofactor distances are not increased above 14 Å, ET will generally not be rate-limiting. In this paper, we describe detailed experiments on *E. coli* fumarate reductase (Frd) that provide a foundation upon which the relationship between ET/catalytic rates and reduction potentials can be built.

Fumarate reductase catalyzes the two-proton, two-electron reaction shown in eq 1:

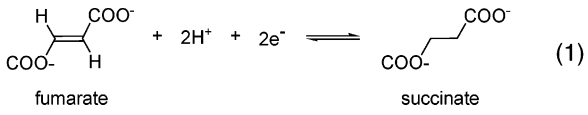

(1)

This enzyme is closely related to succinate:quinone reductase (SQR), also known as succinate dehydrogenase or mitochondrial Complex II, which is a component of the citric acid cycle and the aerobic respiratory chain.[8] The active site is similar to fumarate reductases from *Wolinella succinogenes*[9] and the *Shewanella* genus (known as flavocytochrome c_3 (Fcc_3)).[10,11] The heterotetramer FrdABCD shown in Figure 1 contains a covalently bound flavin adenine dinucleotide (FAD) in the FrdA subunit, three Fe−S clusters ([2Fe−2S], [4Fe−4S], and [3Fe−4S] in increasing distance from the FAD) in the FrdB subunit, and two menaquinone binding sites in the membrane-intrinsic domain (FrdCD). This study focuses on the soluble FrdAB domain, which adsorbs at a pyrolytic graphite "edge" (PGE)

[†] University of Oxford.
[‡] VA Medical Center and University of California.

(1) Ohnishi, T. *Biochim. Biophys. Acta* **1998**, *1364*, 186−206.
(2) Yankovskaya, V.; Horsefield, R.; Törnroth, S.; Luna-Chavez, C.; Miyoshi, H.; Léger, C.; Byrne, B.; Cecchini, G.; Iwata, S. *Science* **2003**, *299*, 700−704.
(3) Zhang, Z.; Huang, L.; Shulmeister, V. M.; Chi, Y.-I.; Kim, K. K.; Hung, L.-W.; Crofts, A. R.; Berry, E. A.; Kim, S.-H. *Nature* **1998**, *392*, 677−684.
(4) Pershad, H. R.; Duff, J. L. C.; Heering, H. A.; Duin, E. C.; Albracht, S. P. J.; Armstrong, F. A. *Biochemistry* **1999**, *38*, 8992−8999.
(5) Guigliarelli, B.; Magalon, A.; Asso, M.; Bertrand, P.; Frixon, C.; Giordano, G.; Blasco, F. *Biochemistry* **1996**, *35*, 4828−4836.
(6) Ohnishi, T.; Moser, C. C.; Page, C. C.; Dutton, P. L.; Yano, T. *Structure* **2000**, *8*, R23−R32.
(7) Page, C. C.; Moser, C. C.; Chen, X.; Dutton, P. L. *Nature* **1999**, *402*, 47−52.
(8) Cecchini, G.; Schröder, I.; Gunsalus, R. P.; Maklashina, E. *Biochim. Biophys. Acta* **2002**, *1553*, 140−157.
(9) Lancaster, C. R. D.; Kröger, A.; Auer, M.; Michel, H. *Nature* **1999**, *402*, 377−386.
(10) Taylor, P.; Pealing, S. L.; Reid, G. A.; Chapman, S. K.; Walkinshaw, M. D. *Nat. Struct. Biol.* **1999**, *6*, 1108−1112.
(11) Leys, D.; Tsapin, A. S.; Nealson, K. H.; Meyer, T. E.; Cusanovich, M. A.; Van Beeumen, J. J. *Nat. Struct. Biol.* **1999**, *6*, 1113−1117.

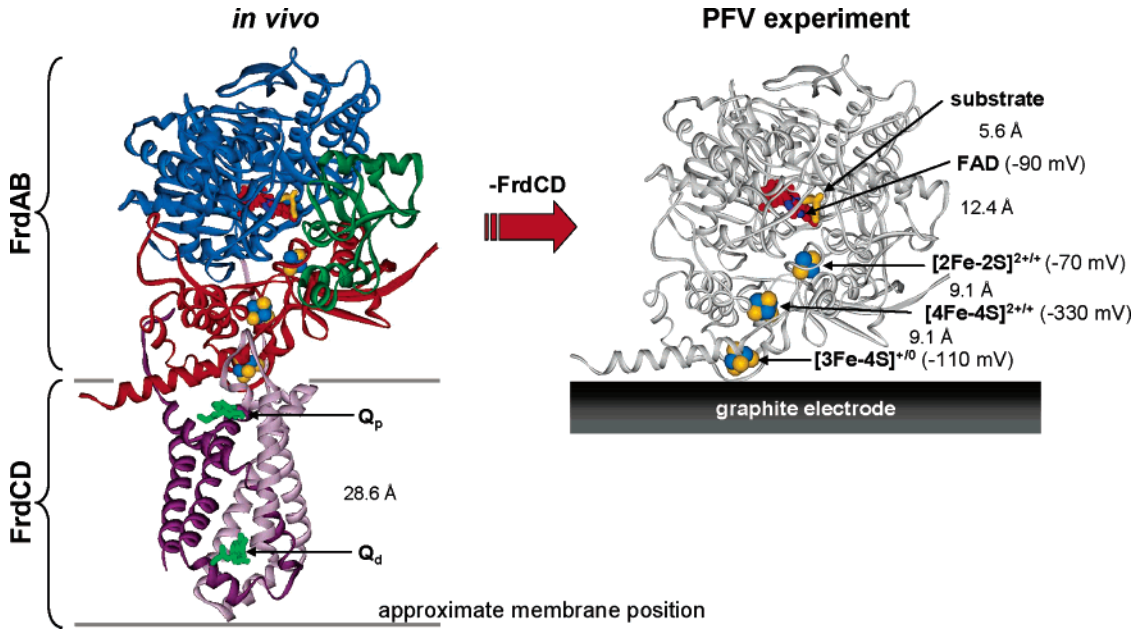

Figure 1. Crystal structure of *E. coli* FrdABCD in the membrane (left) and cartoon suggesting how FrdAB must be oriented on an electrode in order to exhibit the electron-transfer rates that are observed (right). On the left, FrdA is shown in blue (FAD binding domain) and green (mobile capping domain); FrdB (iron−sulfur protein) is in red; FrdC and FrdD (membrane-bound subunits removed by genetic manipulations, as described in Materials and Methods) are in light and dark purple, respectively. The molecule in the substrate binding pocket is the inhibitor oxaloacetate. The proximal and distal menaquinone molecules are denoted by Q_p and Q_d, respectively. Protein Data Bank (PDB) code: 1L0V.[14] Distances are the shortest between the edge of the conjugated rings for the menaquinones and FAD, the atoms in (not ligated to) the Fe−S clusters, and the N5 of FAD to the C2 of OAA. Reduction potentials measured using PFV at 25 °C, pH 7 (mixed buffer), as described in the text.

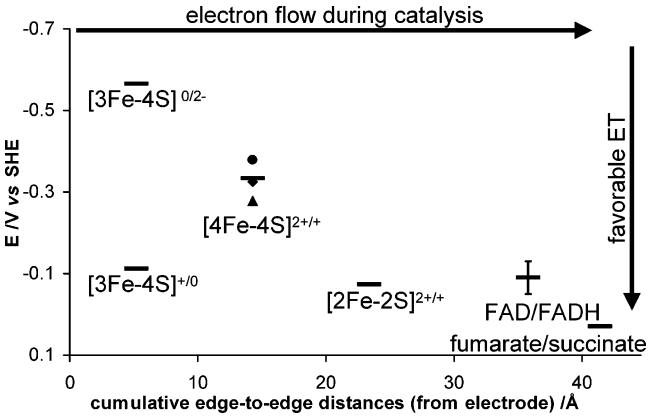

Figure 2. Reduction potentials of the cofactors within WT FrdAB and their distance along the ET chain from the electrode (pH 7, 25 °C). [4Fe−4S] potentials for the mutants are also shown: L153C (▲), Y155S (●), L153C/Y155S (◆) (potentials of other centers in mutants do not vary significantly from WT). The two one-electron potentials of the FAD reduction predicted to lie close to the upper and lower limits of the vertical line placed over the FAD/FADH$_2$ potential (estimated on the basis of n_{app} = 1.8, so $\Delta E = -80$ mV). The reduction potential of the hyper-reduced [3Fe−4S]$^{0/2-}$ couple is shown for pH 5. Distances are as shown in Figure 1.

electrode on which it displays a high rate of catalytic activity for fumarate reduction.[12,13]

The crystal structure[14] suggests that all three Fe−S clusters are critical components of a near linear "wire" to transfer electrons from the *electron entry point* at the proximal quinone-binding site (Q_p) in the membrane-bound FrdCD domains to the *buried* FAD active site in FrdA. During a protein film voltammetry (PFV) experiment, the PGE electrode replaces the quinone as the electron donor. As indicated also in Figure 1 (and supported by results of this investigation), when FrdAB is adsorbed at an electrode, it is extremely likely that the electrons enter the enzyme at the relatively exposed [3Fe−4S] cluster and travel via the [4Fe−4S] cluster to reach the deeply buried [2Fe−2S] cluster and FAD. Bypassing any cluster would require electrons to tunnel distances far greater than 14 Å (the edge−edge distance from the [3Fe−4S] to the [2Fe−2S] cluster is 20.3 Å, and from the [4Fe−4S] cluster to the FAD is 19.4 Å). However, their reduction potentials do not provide a smooth series of exergonic ET steps to the active site. The [4Fe−4S] cluster, positioned between the [3Fe−4S] and the [2Fe−2S] clusters, has a reduction potential of −330 mV, which is more than 200 mV lower (therefore much more difficult to reduce) than that of the other two clusters ([3Fe−4S] = −110 mV, [2Fe−2S] = −70 mV).[15] The situation is depicted in Figure 2, which includes data for the cooperative two-electron reduction of the FAD and for the two-electron hyper-reduction couple of the [3Fe−4S] cluster, as identified in small ferredoxins.[16−19]

(12) Sucheta, A.; Cammack, R.; Weiner, J.; Armstrong, F. A. *Biochemistry* **1993**, *32*, 5455−5465.
(13) Heering, H. A.; Weiner, J. H.; Armstrong, F. A. *J. Am. Chem. Soc.* **1997**, *119*, 11628−11638.
(14) Iverson, T. M.; Luna-Chavez, C.; Cecchini, G.; Rees, D. C. *Science* **1999**, *284*, 1961−1966.
(15) It was suggested that the microscopic reduction potential of the [4Fe−4S] cluster is not as low as the macroscopic value, due to anti-cooperative interactions between the clusters (Salerno, J. C. *Biochem. Soc. Trans.* **1991**, *19*, 599−605). However, studies on mutants in which the potentials of the [2Fe−2S] and [3Fe−4S] clusters were altered showed that the intrinsic midpoint potential of the [4Fe−4S] cluster is still below −240 mV, which should provide a significant barrier to ET in either direction (ref 41 and Werth, M. T.; Cecchini, G.; Manodori, A.; Ackrell, B. A. C.; Schroder, I.; Gunsalus, R. P.; Johnson, M. K. *Proc. Natl. Acad. Sci. U.S.A.* **1990**, *87*, 8965−8969).
(16) Armstrong, F. A.; Butt, J. N.; George, S. J.; Hatchikian, E. C.; Thomson, A. J. *FEBS Lett.* **1989**, *259*, 15−18.
(17) Shen, B.; Martin, L. L.; Butt, J. N.; Armstrong, F. A.; Stout, C. D.; Jensen, G. M.; Stephens, P. J.; La Mar, G. N.; Gorst, C. M.; Burgess, B. K. *J. Biol. Chem.* **1993**, *268*, 25928−25939.
(18) Duff, J. L. C.; Breton, J. L. J.; Butt, J. N.; Armstrong, F. A.; Thomson, A. J. *J. Am. Chem. Soc.* **1996**, *118*, 8593−8603.

E. coli FrdB	CINCG**L**C**Y**AACP	159
E. coli SdhB	CILCA**C**C**S**TSCP	160
W. succinogenes FrdB	CIECG**C**C**I**AACG	162
Bovine SdhB	CILCA**C**C**S**TSCP	169
Human SdhB	CILCA**C**C**S**TSCP	197
	# # #	

Figure 3. Section of the sequence alignment for the Fe−S subunit from various fumarate reductases and succinate dehydrogenases. Residues that were mutated in this study are underlined, # indicates three of the four cysteines directly ligating the [4Fe−4S] cluster (fourth not shown). Sequences aligned using ClustalW from the European Bioinformatics Institute (www.ebi.ac.uk/clustalw/).

In a recent study of electron relays in FrdAB and Fcc_3. we explored the use of square-wave voltammetry to measure the driving force dependence of the redox cycling of the FAD. The results suggested that ET along the relay could be rate-limiting in FrdAB.[20] In this study, we have used PFV to measure the long-range ET and catalytic activities of FrdAB variants in which the [4Fe−4S] reduction potential has been altered over a 100 mV range. Using PFV, ET can be driven, controlled, and measured over a continuous range of driving force. Not only can rates of ET and active-site redox cycling be determined in such a way that the external driving force is factored out but also it is possible to detect transitions in catalytic activity as the electrode potential passes through critical regions, such as redox couples of specific centers. We have investigated the role of the $[3Fe-4S]^{+/0}$ cluster by causing it, electrochemically, to utilize instead an alternative low potential redox couple ($0/1^{-}/2^{-}$) that ought to provide an energetically more-favorable "downhill" relay (Figure 2).[18,19] We have investigated the role of the [4Fe−4S] cluster by mutating two residues, each located close to the coordinating cysteines, to mimic the homologous sequence of *E. coli* succinate dehydrogenase (Figure 3) for which the [4Fe−4S] potential is approximately 100 mV higher.[21] For this, three mutants were prepared: leucine B153 was mutated to cysteine (L153C); tyrosine B155 was mutated to serine (Y155S); and a "double" mutant (L153C/Y155S) was prepared to combine both mis-sense mutations.

Materials and Methods

Enzyme Preparation. The recombinant soluble domain, FrdAB, from *E. coli* containing an eight amino acid extension (Leu-Glu-6xHis) was constructed and expressed in *E. coli* from plasmid pFAB-HT, as described previously.[22] Site-directed mutants were constructed using plasmid pFAB-HT as a template, utilizing the ExSite PCR mutagenesis kit from Stratagene (La Jolla, CA). Wild-type and mutant forms of FrdAB were purified by a modification of previous methods.[22] Cells were grown and enzymes expressed as before, but the harvested cells were suspended in buffer A (pH 7.0, 50 mM potassium phosphate, 20 mM imidazole, 1% (w/v) glycerol), with one Complete Protease Inhibitor Tablet (ethylenediaminetetraacetic acid (EDTA) free) from Roche (Indianapolis, IN) added per 50 mL of suspended cells. The cells were then disrupted by two passages through an Avestin homogenizer at 15 000 PSI at 4 °C. Cells and membranes were removed by centrifugation at 120 000*g* in a Beckman Ti60 rotor for 35 min. The supernatant was filtered through a 0.45 μm syringe filter and applied to a Ni affinity column (2 × 11 cm; Qiagen Chatsworth, CA) equilibrated with buffer A. The column was washed with three volumes of buffer A until no more protein eluted, then with buffer B (pH 7.0, 50 mM potassium phosphate, 0.2 M imidazole, 1% glycerol) to elute the enzyme. Fractions were pooled, brought to 60% ammonium sulfate saturation, incubated on ice for 30 min, and then centrifuged at 12 000*g* for 10 min. The precipitated enzyme was stored at −80 °C.

Prior to electrochemistry, FrdAB samples were further purified in an anaerobic glovebox (Belle Technology, O_2 < 4 ppm). The pellets were dissolved in a minimum of buffer (20 mM HEPES (4-(2-hydroxyethyl)piperazine-1-ethanesulfonic acid) or PIPES (piperazine-1,4-bis(2-ethanesulfonic acid), 0.1 mM ethyleneglycol-bis(2-amino-ethylether)-*N*,*N*,*N*′,*N*′-tetraacetic acid (EGTA), 0.5 mM DTT (dithio-threitol), and 10% w/v glycerol), and the ammonium sulfate was removed on a desalting column (PD10, Pharmacia). The samples were then purified by ion exchange on a Mono Q column (Pharmacia) equilibrated with the same buffer. The enzyme eluted at ∼50% of the 0−0.5 M NaCl gradient and was stored under liquid nitrogen.

Solution Kinetics. All enzyme activities were measured at 25 °C, using buffers containing 30 mM Bis/Tris/propane and 0.1 mM EDTA, at pH 6.0, 7.0, and 8.5. Fumarate reductase activity was assayed by monitoring the fumarate-dependent reoxidation of reduced benzyl viologen (BV, $A_{555nm} = 9.2\ mM^{-1}\ cm^{-1}$, $E^{0'} = -359$ mV at pH 8[23]) under anaerobic conditions. A cuvette with 3 mL of buffer containing 10 mM glucose and 0.1 mg/mL of glucose oxidase and catalase was equilibrated for 5 min to eliminate O_2, and then 0.2 mM BV, 10 mM fumarate ($\gg K_M$), and dithionite (from solution) were added. The reaction was initiated by adding 2−5 μL of protein. Succinate: ferricyanide reductase activity was assayed under aerobic conditions with 0.5 mM $K_3Fe(CN)_6$ ($A_{420nm} = 1\ mM^{-1}\ cm^{-1}$) and 20 mM succinate.

Electrochemistry. Removal of the membrane-intrinsic subunits (FrdCD) renders the enzyme (FrdAB) more prone to damage by O_2.[24] For this reason and to avoid O_2 being reduced at the electrode, thus complicating the voltammetry, all experiments were carried out under N_2 in a glovebox (O_2 < 4 ppm, Vacuum Atmospheres or M. Braun). All chemicals were of the highest grade (Sigma-Aldrich). Solutions for fast-scan cyclic voltammetry (deionized water; 18 MΩ cm) contained 20 mM PIPES (pH 7)[25] or TAPS (*N*-[tris(hydroxymethyl)-methyl]-3-aminopropanesulfonic acid, pH 8 and 8.5). Catalytic voltammograms were recorded with mixed buffers comprising 20 mM in each of citrate, MES (2-morpholinoethanesulfonic acid), PIPES, and TAPS. Experiments to determine the effect of hyper-reducing the [3Fe−4S] cluster were performed in 20 mM citrate buffer. All solutions also contained 100 mM NaCl as extra supporting electrolyte.

The glass electrochemical cell[20] was maintained at 25 °C, and the potentials (recorded versus a saturated calomel electrode) were converted to the standard hydrogen electrode (SHE) scale at the experimental temperature.[26] A Faraday cage (1 cm mesh) was used to decrease electrical noise. The PGE rotating disk electrode (∼3 mm^2 surface area, constructed as described previously[12]) was polished with 1 μm alumina (Buehler, USA), immediately before smearing 2 μL of polymyxin B sulfate (Sigma, 20 mg ml^{-1}) and 2−8 μL of enzyme sample (∼10 μM FrdAB) over the graphite surface. Polymyxin serves as a co-adsorbate to stabilize the enzyme film on the electrode. After

(19) Hirst, J.; Jameson, G. N. L.; Allen, J. W. A.; Armstrong, F. A. *J. Am. Chem. Soc.* **1998**, *120*, 11994−11999.
(20) Jeuken, L. J. C.; Jones, A. K.; Chapman, S. K.; Cecchini, G.; Armstrong, F. A. *J. Am. Chem. Soc.* **2002**, *124*, 5702−5713.
(21) Condon, C.; Cammack, R.; Patil, D. S.; Owen, P. *J. Biol. Chem.* **1985**, *260*, 9427−9434.
(22) Léger, C.; Heffron, K.; Pershad, H. R.; Maklashina, E.; Luna-Chavez, C.; Cecchini, G.; Ackrell, B. A. C.; Armstrong, F. A. *Biochemistry* **2001**, *40*, 11234−11245.
(23) Clark, W. M. *Oxidation−Reduction Potentials of Organic Systems*; Waverly Press: Baltimore, MD, 1972.
(24) Ackrell, B. A. C.; Johnson, M. K.; Gunsalus, R. P.; Cecchini, G. In *Chemistry and Biochemistry of Flavoenzymes*; Müller, F., Ed.; CRC Press: Boca Rato, Florida, 1992; Vol. 3, pp 229−297.
(25) The presence of HEPES (Sigma-Aldrich) in the buffer consistently gave distorted electrochemical data at pH 7 above 20 V s^{-1}, and so PIPES was used for these experiments instead. This effect was not observed in previous studies (see ref 22) and may have been caused by a contaminant.
(26) Bard, A. J.; Faulkner, L. R. *Electrochemical Methods: Fundamentals and Applications*, 2nd ed.; John Wiley & Sons: New York, 2001.

inserting the electrode into the cell solution, the potential was cycled twice between 0.24 and −0.65 V at 0.02 V s^{-1}, and the quality of the signals was examined before commencing the experiment. All potential cycles were initiated from the high potential limit, and checks showed that identical results were obtained when the cycle was started after poising at low potential (excluding those using oxaloacetate (OAA), see later). Voltammetry was recorded using an Autolab system (EcoChemie, Utrecht, The Netherlands) equipped with SCANGEN and ADC750 (analogue−digital converter) modules for fast scan rates (>1 V s^{-1}) and an ECD (electrochemical detection) module to improve current sensitivity at slower scan rates (<0.1 V s^{-1}). Uncompensated resistance was minimized using the positive-feedback iR compensation feature.

The reduction potentials for the FAD and [4Fe−4S] cluster measured at slow scan rates (<1 V s^{-1}) are precise within 5 mV, and those at higher rates have errors of ±10 mV. Potentials of the [3Fe−4S] and [2Fe−2S] clusters were obtained by deconvoluting the complex signal with assignments guided by potentiometric data[27] and thus have a greater degree of error (±20 mV). All data were Fourier-filtered to remove noise, and the non-Faradaic (baseline) current was subtracted using an in-house program developed by Dr. C. Léger and Dr. H. A. Heering.

Experiments to examine the boost in catalytic activity at potentials below the [4Fe−4S] reduction potential were performed at high substrate concentrations (5 mM fumarate) corresponding to 99% occupation of active sites (K_M = 20 μM for FrdABCD,[28] 50 μM for WT His-tag FrdAB, this work). It was assumed that the K_M values of the mutants were not significantly different to WT since there was no perturbation of the FAD potential (vide infra) to indicate any alteration of the active site. Variations in K_M would, in any case, have little effect with substrate in large excess. The electrode was rotated (EG&G M636 electrode rotator, Princeton Applied Research) at speeds sufficiently fast (2000 rpm) that the wave shape was independent of rotation rate and thus not limited by substrate transport to the electrode surface.

In studies with the inhibitor OAA, the concentration was chosen so that OAA was bound to the active site when the FAD was oxidized but was released when the FAD was reduced. Since binding of OAA to Frd is slow,[13,29] all experiments included an oxidative pre-poise at +0.24 V for 30 s to ensure that the cycle started from a defined state of equilibrium (in this case, all cofactors were oxidized).

Results

Reduction Potentials. Nonturnover (i.e., without substrate) cyclic voltammograms for WT FrdAB and L153C, Y155S, and L153C/Y155S mutants were recorded at 25 °C, producing peaks corresponding to the cycle of reduction and reoxidation of the four cofactors (flavin and three Fe−S clusters). Figure 4 shows an overlay of these data at pH 7. In cyclic voltammetry, the reduction potential for a redox couple is given by the average of the oxidation and reduction peak potentials. The outer light-blue voltammogram displays the raw data for WT enzyme; the inner voltammograms show the data for the WT and three mutants, with the background capacitance removed (offset for clarity).

As described previously,[12,13] two sets of signals are evident in each case: the larger envelope at high potential is dominated by the sharp two-electron FAD signal which overlays signals due to two one-electron couples, that is, the $[2Fe-2S]^{2+/+}$ and $[3Fe-4S]^{+/0}$ couples (which are easily resolved by deconvolution); the smaller, low potential peak corresponds to the one-

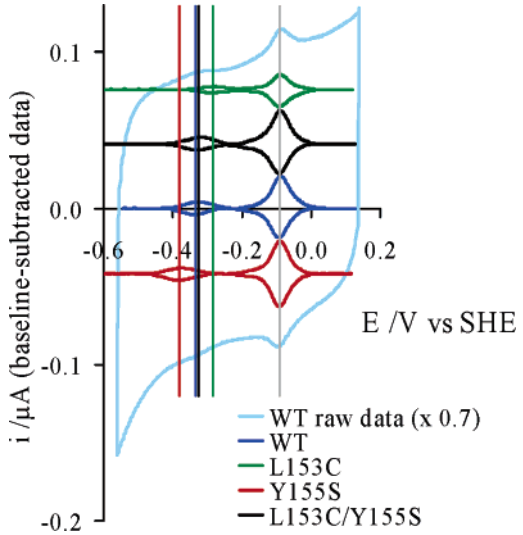

Figure 4. Cyclic voltammograms comparing WT FrdAB and [4Fe−4S] mutants at pH 7, 25 °C, scan rate = 20 mV s^{-1}. Both raw and baseline-subtracted data are presented for WT, and the baseline-subtracted voltammograms are shown for all of the mutants. The current scale applies only to the baseline-subtracted (not the raw data), and voltammograms for the mutants have been offset on the current scale for clarity. Note that the film coverage of mutant L153C was lower than that for other species, thus causing smaller peaks. Arrows indicate the direction of scan, and vertical lines represent the reduction potentials of the FAD (gray) and [4Fe−4S] clusters (shown in same colors as the data from which they arise).

electron reduction and oxidation of the $[4Fe-4S]^{2+/+}$ cluster.[12] The intensity of the FAD signal reflects the proportionality of peak height (i_p) to the square of the number of electrons transferred cooperatively (n_s is the stoichiometric number of electrons transferred, and n_{app} is the empirical measure of cooperativity). Thus for $n_s = 2$, the flavin semiquinone radical is inherently unstable for the condition $1 \le n_{app} \le 2$. The half-height peak width (δ) is inversely proportional to the number of electrons cooperatively transferred. The relevant equations are 2 and 3, which assume a homogeneous sample on the electrode:

$$i_p = n_s n_{app} F^2 \nu A\Gamma/4RT \quad (2)$$

$$\delta = 3.53RT/n_{app}F \quad (3)$$

where ν is the scan rate, A the electrode surface area, Γ the electroactive coverage of enzyme on the electrode, and F, R, and T have their usual meanings.[30] Thus, in the limit of a fully cooperative two-electron transfer, the FAD peaks are expected to have 4 times the height and half the width of the one-electron Fe−S cluster peaks. In fact, the value $n_{app} = 1.8$ produces the best fit for both pH 7.0 and 8.5 after deconvolution; therefore, the FAD behaves as a cooperative two-electron center. Clearly, the mutations altering the [4Fe−4S] cluster binding region in FrdB have not altered the two-electron reduction potential of the FAD in FrdA (−90 mV at pH 7, 25 °C), and this is true over the entire pH range of 5−9 where the lines (linear, with slope between −24 and −29 mV/pH unit, consistent with a two-electron, one-proton transfer) are identical in each case (not shown). It is therefore highly unlikely that the FrdB mutations have altered the FAD environment. By contrast, the position of

(27) Cammack, R.; Patil, D. S.; Weiner, J. H. *Biochim. Biophys. Acta* **1986**, *870*, 545−551.
(28) Schröder, I.; Gunsalus, R. P.; Ackrell, B. A. C.; Cochran, B.; Cecchini, G. *J. Biol. Chem.* **1991**, *266*, 13572−13579.
(29) Ackrell, B. A. C.; Cochran, B.; Cecchini, G. *Arch. Biochem. Biophys.* **1989**, *268*, 26−34.
(30) Armstrong, F. A.; Heering, H. A.; Hirst, J. *Chem. Soc. Rev.* **1997**, *26*, 169−179.

Table 1. Comparison of Equilibrium Reduction Potentials for WT FrdAB and [4Fe−4S] Mutants at 25 °C

species	FAD[d]	$[2Fe–2S]^{2+/+}$ [a]	$[4Fe–4S]^{2+/+}$ [b]	$[3Fe–4S]^{+/0}$ [a]	$[3Fe–4S]^{0/2-}$ pH 5.0
WT pH 7.0	−90 ± 5	−74 ± 20	−333 ± 5	−111	−565 ± 5[c]
WT pH 8.5	−125 ± 5	−92 ± 20	−364 ± 5	−137 ± 20	NA[c]
L153C pH 7.0	−90 ± 5	−62 ± 20	−279 ± 5 (+54)	−108 ± 20	−565 ± 5[c]
Y155S pH 7.0	−91 ± 5	−82 ± 20	−379 ± 5 (−46)	−108 ± 20	−567 ± 5[c]
L153C/Y155S pH 7.0	−89 ± 5	−80 ± 20	−325 ± 5 (+8)	−129 ± 20	−561 ± 5[c]

[a] Value determined by deconvolution, thus producing greater error. Errors are discussed in greater detail in Materials and Methods. [b] Numbers in brackets refer to the difference compared to the WT value. [c] The hyper-reduced [3Fe−4S] cluster is only evident for pH < 7. All of these values are recorded at pH 5.0, as described in Materials and Methods. [d] Previous experiments were carried out at lower temperatures, which gave more positive reduction potentials.

the [4Fe−4S] cluster signal is distinctly altered; at pH 7, the L153C potential is shifted +54 mV with respect to WT, Y155S is shifted −46 mV, and the L153C/Y155S mutant is shifted +8 mV (see also Table 1).

Apparent Electron-Transfer Rates. Owing to its two-electron cooperativity, the FAD signal *dominates* the high potential envelope; thus, the variation of oxidative and reductive peak positions as a function of scan rate yields the rate that the FAD *exchanges* two electrons with the electrode, that is, without a net driving force. This will be referred to as the "apparent ET exchange rate constant" (k_0') of the FAD and can be estimated using Butler−Volmer theory.[20] More correctly, k_0' is the rate of redox cycling of the FAD cofactor, using the Fe−S relay shown in Figure 1. The sharp peaks in both directions that arise from a cooperative, two-electron transfer suggest also that k_0' is identified with the rate-determining *first* electron in or out of the center (see later). This may be qualified further; ideally, the pH dependence of the two-electron reduction potential requires that one proton is also exchanged with solvent within the time of the cycle; however (see Discussion), this applies only if the reduction potential measured at high scan rate is the same as that measured at equilibrium. The smaller, low potential signal due to the [4Fe−4S] cluster is tracked in similar fashion, and the ET exchange rate constant can also be calculated, although the error is now much larger.[31] Thus, FrdAB is an excellent system to determine the effect of the potentials of the components of an "electron wire" on the ET rate.

Figure 5A shows a plot of the oxidative and reductive peak positions for the dominant FAD component against scan rate (log scale) at two pH values. We have referred to this as a "trumpet plot".[19,30,32] It depicts the pattern of electron exchange and coupled reactions over a range of time domains. At scan rates sufficiently low that the system stays close to electrochemical equilibrium, the oxidation and reduction peaks occur at approximately the same potential (within ∼5 mV at 20 mV s^{-1}). However, as the scan rate is increased, there is an increasingly delayed response to potential change, resulting in the oxidation peaks moving to higher potentials and the reduction peaks to lower potentials; thus, a peak separation develops. A large potential separation at slow scan rates indicates a very slow ET rate, whereas a narrow trumpet plot signifies fast ET. Potential cycles were commenced from the high potential limit (oxidative poise); however, no significant difference was found if cycles were commenced from the low potential limit.

An ideal reversible electron exchange should produce a symmetrical trumpet plot, whereas Figure 5A shows a distinct

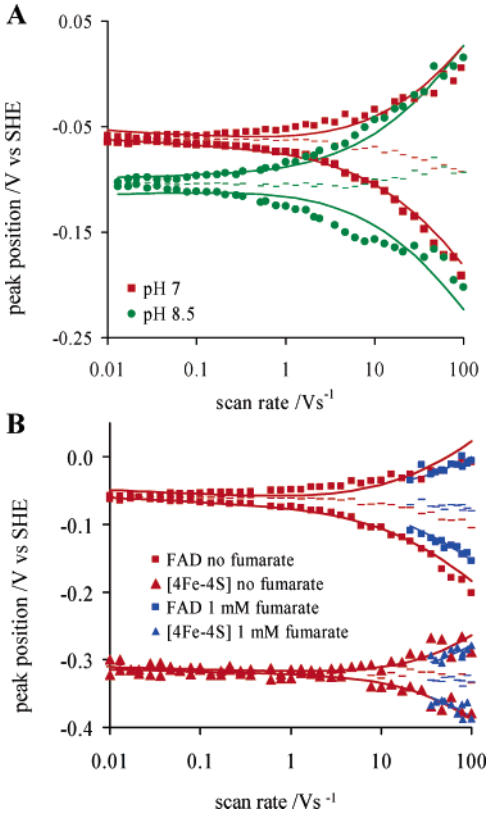

Figure 5. Trumpet plots displaying the response of the reduction potentials of WT FrdAB to fast scan rates. The top half of each trumpet plot shows the oxidation peak positions, while the lower half represents the reduction peaks. (A) Comparison of trumpet plots of the FAD signal at pH 7 (red squares) and 8.5 (green circles) at 25 °C. The averages of the oxidation and reduction peaks are each shown by a dash, and solid lines indicate the fit to Butler−Volmer kinetics. (B) Trumpet plots for both the FAD (squares) and [4Fe−4S] cluster (triangles) signals in the absence (red symbols) and presence (blue symbols) of 1 mM fumarate, pH 7, 25 °C.

downward distortion at pH 7 (a −33 mV shift between 0.01 and 78 V s^{-1}) and a slight upward trend for pH 8.5 (+9 mV) as the scan rate is increased above 10 V s^{-1}. Previous studies at pH 7.3[13] were limited to scan rates of ≤20 V s^{-1} and did not reveal the extent of this effect. At high scan rates, the data for pH 7 and 8.5 begin to converge, and this will be discussed later.

For WT FrdAB, allowing for the nonideal downward slope (an empirical correction, not a manipulation of the Butler−Volmer model), the two-electron k_0' at pH 7 for the FAD is 800 s^{-1}, whereas at pH 8.5, the two-electron k_0' is 450 s^{-1}. For reasons discussed later, these probably represent lower limits. The one-electron k_0' for the [4Fe−4S] cluster at pH 7 was estimated at 800 s^{-1} (no attempt was made to determine k_0' for the [4Fe−4S] cluster at pH 8.5, due to the smaller film coverage). These rate constants are summarized in Table 2. The FAD reduction peaks for high scan rates (>20 s^{-1}) at pH 8.5

(31) Since deconvolution assumes equilibrium conditions (and thus slow scan rates), the ET rates to the [3Fe−4S] and [2Fe−2S] clusters cannot be measured in this way.

(32) Léger, C.; Elliott, S. J.; Hoke, K. R.; Jeuken, L. J. C.; Jones, A. K.; Armstrong, F. A. *Biochemistry* **2003**, *42*, 8653−8662.

Table 2. Comparison of Apparent ET Exchange Rates (k_0') between the Electrode and the Cofactors in WT FrdAB and [4Fe−4S] Mutants under Various Conditions at 25 °C

species conditions	k_0' (FAD)/s^{-1} [a]	k_0' ([4Fe–4S])/s^{-1} [a]
WT pH 7	800 ± 100	800 ± 250
WT pH 8.5	450 ± 100	ND[b]
WT pH7, 1 mM fumarate	1550 ± 100	950 ± 250
L153C pH 7	900 ± 300	ND[b]
Y155S pH 7	750 ± 250	650 ± 250
L153C/Y155S pH 7	850 ± 200	650 ± 250

[a] The k_0' values from the electrode to the cofactors of FrdAB were calculated by fitting the trumpet plot data to Butler−Volmer kinetics. [b] Data were not of sufficient quality to determine a value.

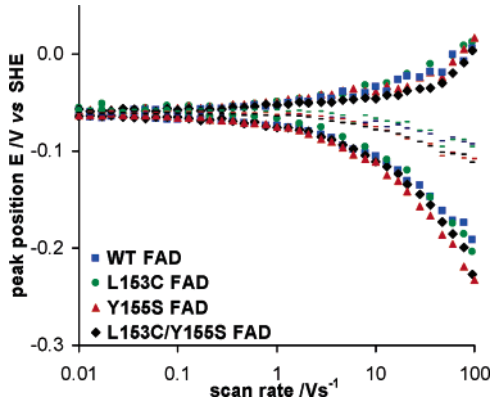

Figure 6. Overlay of trumpet plots at pH 7, 25 °C, showing the scan rate dependence of the FAD signal for WT and three mutants of FrdAB. Dashed line represents the average reduction potential.

showed significant broadening, contributing to the scatter of data points. Further studies and comparisons between mutants and WT enzyme were carried out at pH 7 to avoid this complication.

It has been shown previously that a trumpet plot can be obtained in the presence of substrate once the scan rate is sufficiently fast to "outrun" catalysis.[33] That is, catalytic waves (see later, and Figure 7) revert to peaks (similar to those in Figure 4) when the electrons used to reduce the FAD are returned to the electrode either before they pass on to the fumarate or before the succinate product can leave. The trumpet plot now displays the redox properties of the enzyme−substrate complex. Figure 5B shows a comparison between the trumpet plots of the FAD and [4Fe−4S] cluster signals of WT FrdAB (pH 7), in the presence and absence of saturating fumarate concentrations. Peaks become evident at scan rates above ~20 V s^{-1} for the FAD and ~36 V s^{-1} for the [4Fe−4S] cluster. Over many experiments, it was consistently observed that the data points obtained in the presence of fumarate lie *inside* the data points obtained in the absence of fumarate (i.e., the peak separation is always smaller when substrate is present). The ET exchange rate constants thus estimated were $k_0' = 1500$ s^{-1} (FAD) and 950 s^{-1} ([4Fe−4S] cluster). For FAD, this is almost a doubling in rate compared to the ET cycling rate without fumarate, but for the [4Fe−4S] cluster, it is only an increase of ~20% and well within the large error margin. The fact that the average reduction potential of the fumarate-bound signals is close to that of the substrate-free enzyme (it increases by only ~10 mV) shows there is just a small preference for fumarate to bind to the reduced rather than the oxidized form of the FAD.

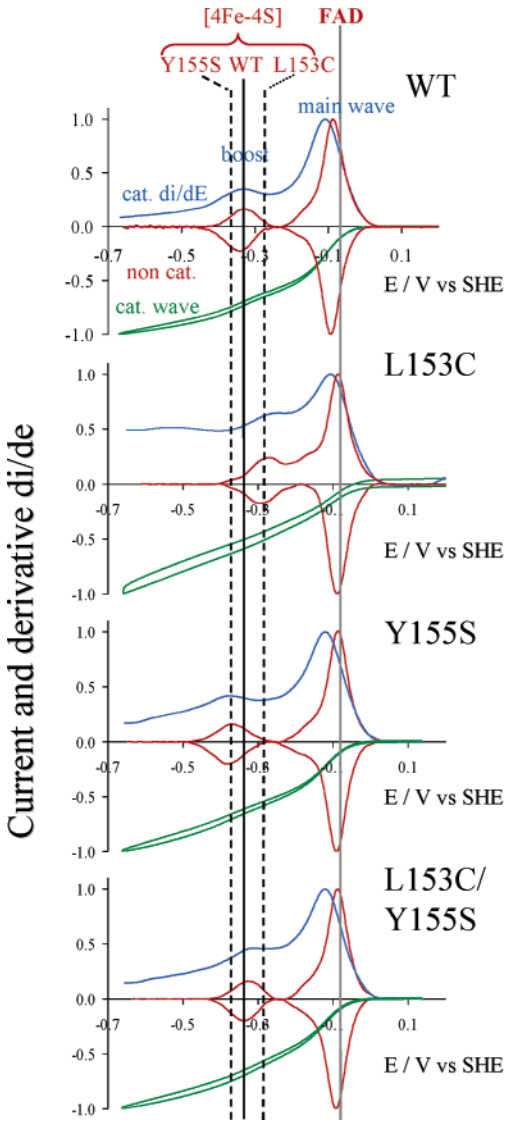

Figure 7. Comparison of the normalized baseline-subtracted noncatalytic signals (red), catalytic wave (green), and first derivative (blue) from WT FrdAB and three [4Fe−4S] mutants. The vertical lines indicate the position of the noncatalytic FAD and [4Fe−4S] cluster signals from each species and show the close correspondence between the potentials of these cofactors and the maxima in the first derivative of the catalytic waves (L153C/Y155S not shown for clarity since its potential is close to that of WT). Other conditions: pH 7.0 with scan rate of 20 mV s^{-1} for all data, catalytic data included 5 mM fumarate with electrode rotation rate of 2000 rpm. For data recorded on different days, the potential was calibrated on the FAD signal (maximum adjustment 5 mV). The derivative was computed for the reductive half-wave and was also Fourier-filtered to eliminate noise.

The overlaid trumpet plots for the [4Fe−4S] mutants and WT at pH 7 (Figure 6) shows that the apparent exchange rate constant of the FAD is not significantly altered by the mutations: k_0' values are 750 s^{-1} (Y155S), 850 s^{-1} (L153C/Y155S), and 900 s^{-1} (L153C) (compared to 800 s^{-1} for WT). The decrease in potential of the reduction peak as the scan rate is increased is reproducibly slightly greater for the Y155S mutant. The [4Fe−4S] data show considerable scatter, but a k_0' value of 650 s^{-1} was estimated for both Y155S and L153C/Y155S variants (compared to 800 s^{-1} for WT). The coverage of L153C was consistently smaller than that for the other mutants; consequently, combined with the difficulty of cleanly separating the FAD and [4Fe−4S] cluster peaks at high scan rates (where both peaks are broadened, compounding their

(33) Jones, A. K.; Camba, R.; Reid, G. A.; Chapman, S. K.; Armstrong, F. A. *J. Am. Chem. Soc.* **2000**, *122*, 6494−6495.

Table 3. Comparison of Maximal Fumarate and Succinate Turnover Rates for WT FrdAB and [4Fe−4S] Mutants at Varying pH at 25 °C[a]

	Fumarate Turnover Rates/s^{-1}			Succinate Turnover Rates/s^{-1}		
	pH 6.0	pH 7.0	pH 8.5	pH 6.0	pH 7.0	pH 8.5
WT	450	350	190	3.5	9.2	22
L153C	190	208	100	0.85	3.6	10
Y155S	820	780	340	2.0	11	27
L153C/Y155S	380	440	220	1.3	4.3	18

[a] All data were obtained from solution assays as described in the text and are quoted per fumarate molecule reduced or succinate molecule oxidized (i.e., per two electrons).

proximity in potential), the k_0' value for the [4Fe−4S] cluster was not determined for this mutant.

Catalytic Rates Measured in Solution. Results of conventional solution assays shown in Table 3 are consistent with a strong catalytic bias toward fumarate reduction; fumarate reduction rates for WT (350 s^{-1}) are almost 40-fold those for succinate oxidation (9 s^{-1}) at pH 7. They also show that the rate of fumarate reduction is highest at low pH values where succinate oxidation is slowest. The L153C mutant, which has the highest [4Fe−4S] potential, catalyzed fumarate reduction at approximately one-half the rate of the WT enzyme, while the "low potential mutant" Y155S reduced fumarate at nearly twice the WT rate. There was no significant change in the rate of fumarate reduction for the double mutant L153C/Y155S, which displays little alteration of the [4Fe−4S] potential. In terms of succinate oxidation, the turnover rate of L153C was approximately $^1/_3$ of WT, and Y155S was slower than at pH 6 (by $^2/_5$), but faster at pH 7 and 8.5. L153C/Y155S oxidizes succinate at approximately one-half the rate of WT.

The Catalytic Rate has an Unusual Potential Dependence. Addition of fumarate to the cell solution transforms the noncatalytic peaks into a catalytic reduction wave (Figure 7, green trace) with a large negative current. The current at any potential is directly proportional to the catalytic rate, thus a cyclic voltammogram reveals how the catalytic rate depends on electrochemical driving force. A sigmoidal waveshape is expected, reaching a maximum current at high driving force, where ET is no longer rate-limiting. Provided substrate mass transport does not limit the current (this is why the electrode is rotated at high speeds), this plateau reflects the turnover rate of the enzyme. The catalytic wave has three regions. The first region (centered at −105 mV for WT at pH 7) is referred to as the "main" wave, after which the current begins to plateau with increasing driving force. However, at approximately −325 mV (again, for WT at pH 7), a second sigmoidal current increase is observed, which is particularly clear for WT and Y155S. We refer to this as the "boost", as it corresponds to an increase in enzymatic activity as the potential is taken down through a particular range. These two activity regions are more clearly defined as local maxima in the first derivative (Figure 7, blue trace). At still lower potential, the voltammogram displays a residual slope, and the current does not reach the predicted plateau, that is, the rate remains dependent on driving force. This is believed to arise from a dispersion of orientations of FrdAB on the electrode, with some enzyme molecules having poorer electronic coupling. This effect has been observed for many enzymes.[34,35]

Catalytic waves were recorded at saturating substrate conditions, and the positions of the main wave and boost were measured for WT and [4Fe−4S] mutants. The rest of Figure 7 shows catalytic voltammograms for each mutant in green, with the first derivative of the catalytic wave in blue and noncatalytic data plotted in red for comparison. It is clear from the vertical lines marking the [4Fe−4S] potentials that there is strong correlation between these potentials and the boost. Figure 8 shows a plot of the reduction potential of the [4Fe−4S] cluster (horizontal axis) against the potential of the boost (vertical axis).

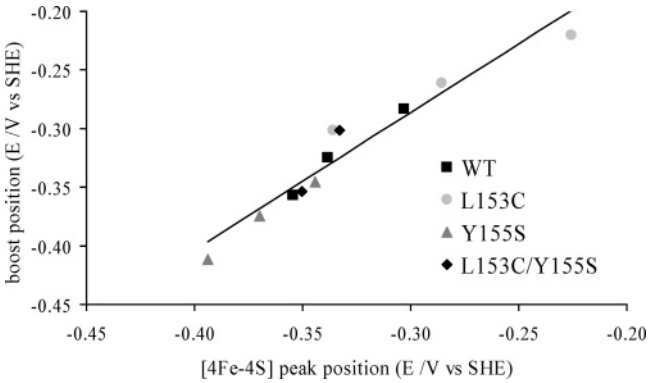

Figure 8. Correlation between the noncatalytic potential of the [4Fe−4S] cluster and the boost in the catalytic wave for FrdAB. The position of the [4Fe−4S] cluster is altered by both mutation and pH (three pH values, 5.9, 7.0, and 8.5, were used for each mutant; the potential decreases with increasing pH). A least-squares regression line is drawn through all points (gradient = 1.2, R^2 = 0.94). Each point is an average of at least two voltammograms for both the noncatalytic and catalytic data. All data were recorded at 25 °C and a scan rate of 20 mV s^{-1}, other conditions are as for Figure 7.

Electrocatalytic kinetic parameters K_M and k_{cat} (the limiting turnover rate under saturating substrate conditions) at pH 7 and 25 °C were determined for the WT enzyme, as described previously. Data are not shown, but the experiment involved measuring the catalytic currents just beyond the boost for a range of fumarate concentrations and electrode rotation rates, then fitting the i_{cat} values obtained (from the intercepts of the Koutecky−Levich plots measured for each fumarate concentration) to eq 4.[12] Here, C is the concentration of fumarate, and other terms have been defined.

$$i_{cat} = \frac{2FA\Gamma k_{cat} C}{(C + K_M)} \qquad (4)$$

This gave the values K_M = 50 μM and k_{cat} = 330 s^{-1}.[36]

Inhibitor Release Rate Depends on Whether [4Fe−4S] is Oxidized or Reduced. Oxaloacetate (OAA) is a competitive inhibitor for both fumarate reductases[37] and succinate dehydrogenases.[38] In its enol tautomer (Figure 9A), it resembles fumarate. In terms of thermodynamics, OAA binds more tightly to oxidized rather than reduced FAD;[13,29] however, the kinetics of binding and release are slow. Experiments carried out with up to 10 mM OAA at 1 mV s^{-1} (without fumarate) showed the

(34) Léger, C.; Jones, A. K.; Albracht, S. P. J.; Armstrong, F. A. *J. Phys. Chem. B* **2002**, *106*, 13058−13063.
(35) Hoke, K. R.; Cobb, N.; Armstrong, F. A.; Hille, R. *Biochemistry* **2004**, *43*, 1667−1674.
(36) This value is lower than we reported in an earlier paper (ref 12); however, all our determinations of these kinetic parameters in recent years (unpublished) give values for k_{cat} at pH 7.0 and 25 °C that are between 350 and 500 s^{-1}.
(37) Cecchini, G.; Ackrell, B. A. C.; Deshler, J. O.; Gunsalus, R. P. *J. Biol. Chem.* **1986**, *261*, 1808−1814.
(38) Ackrell, B. A. C.; Kearney, E. B.; Mayr, M. *J. Biol. Chem.* **1974**, *249*, 2021−2027.

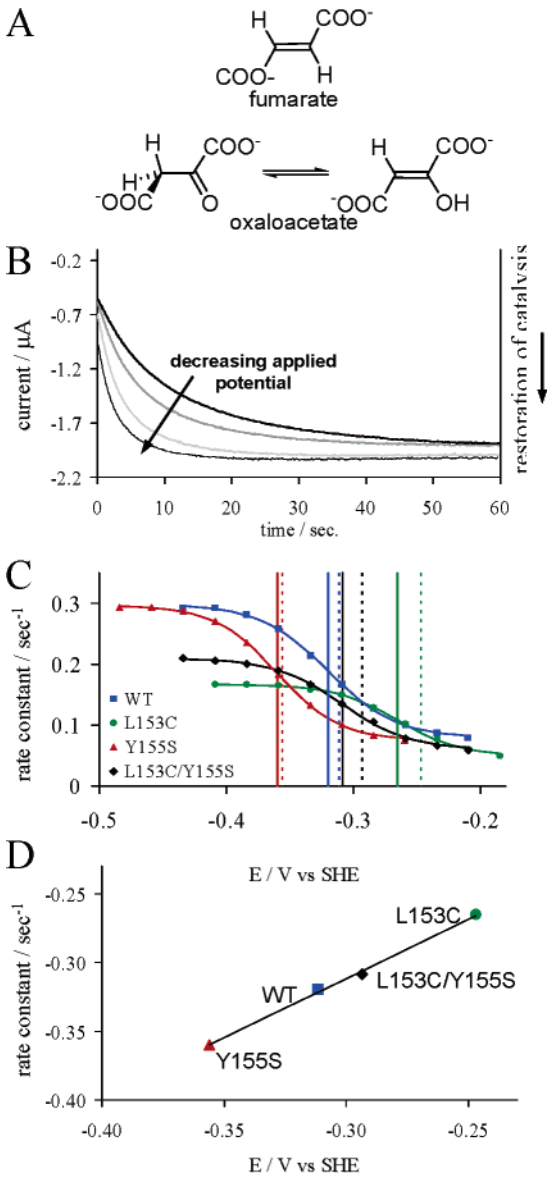

Figure 9. Effect of applied potential on OAA release for WT FrdAB and three mutants. (A) Comparison of the structures of fumarate (substrate) and oxaloacetate (inhibitor, both keto and enol tautomers). (B) Chronoamperometric traces of WT FrdAB showing the recovery of activity (negative current) when reducing potentials are applied (−0.21, −0.284, −0.334, and −0.434 V) after allowing OAA to bind at +0.24 V for 30 s. These data were fitted to a single exponential to extract rate constants at each potential, and these are shown in graph C. (C) Release rate constants (extracted from data analogous to B) as a function of applied potential for WT FrdAB and three [4Fe−4S] mutants. A sigmoid was fitted to the data from each mutant, with the half-wave potential shown with a solid vertical line. The dotted vertical line shows the corresponding $[4Fe-4S]^{2+/+}$ potential under these conditions. (D) Correlation between the reduction potential of the [4Fe−4S] cluster and the half-wave potential of the OAA release curve for WT and three [4Fe−4S] mutants. A least-squares regression line is drawn through all points (gradient = 0.88, $R^2 = 0.999$). All data were recorded at pH 7, 25 °C, 100 μM fumarate, 50 μM OAA, and 1000 rpm.

expected shift in FAD potential (−90 mV), but there was no evidence for any catalytic reduction of OAA. Figure 9B shows the current traces observed for WT FrdAB after stepping the potential from an oxidizing potential (+0.24 V, at which the electrode has been held for 30 s to ensure that OAA is bound) to different negative values (resulting in reduction of FAD, release of OAA, and catalytic activity). In all cases, the rate of current increase (recovery of activity) is slow, whereas in the absence of OAA, there is an essentially instantaneous attainment of maximum activity as the potential is stepped down.

The rate of increase in activity equates with the rate of release of OAA from the active site. Since current is proportional to the amount of active enzyme and recovery of activity is proportional to the amount of inhibited enzyme, these traces can be fitted to a single exponential to extract first-order rate constants, which are independent of electrode coverage. Confirming previous work in this laboratory, we found a strong dependence of the release rate constant of OAA on reduction potential.[13] Fitting to a Nernstian sigmoid produced a width equating to a one-electron reaction ($n = 0.95$). The sigmoid had a half-wave potential of −319 mV, which coincides closely with the $[4Fe-4S]^{2+/+}$ reduction potential (−311 mV)[39] (Figure 9C).

All of the mutants displayed potential-dependent OAA release rates, with each Nernstian sigmoid having similar one-electron widths ($n = 0.96-1.05$). In each case, the half-wave potential is shifted compared to the WT value: L153C by +55 mV, Y155S by −40 mV, and L153C/Y155S by +11 mV, also correlating closely with the [4Fe−4S] potentials (see Table 1). These data are included in Figure 9C, and the correlations between half-wave potentials for OAA release and reduction potentials of the [4Fe−4S] cluster are shown in Figure 9D. At potentials above that of the [4Fe−4S] cluster, the rates are very similar (between 0.05 and 0.08 s^{-1}), but at low potentials, the mutants showed different limiting rate constants for OAA release: 0.29 (WT), 0.29 (Y155S), 0.17 (L153C), and 0.21 s^{-1} (L153C/Y155S). The enhancements of release rates were remarkably similar, and in each case the factor was 3.7 ± 0.2.

Hyper-Reduction of the [3Fe−4S] Cluster. Below pH 7, a relatively sharp, reversible signal is detected at very low potentials in the noncatalytic voltammogram of WT FrdAB and mutants (see CV in Figure 10A and reduction potentials in Table 1). A similar redox couple is widely observed for ferredoxins that contain a [3Fe−4S] cluster and has been explained in terms of a cooperative two-electron process involving the normal one-electron reduced level (0) and one (2^-) that formally contains three Fe(II).[16−19] The ratio of the peak areas in Figure 10A shows that the low potential couple more closely resembles a two-electron process ($n_s \sim 1.6$) at pH 5; the low potential peak is ∼23% of the total peak area (compared to $^2/_7$ or 29% expected from stoichiometry). This unusual "hyper-reduction" involves proton uptake. Here, the potential dependence of −57 mV/pH unit gradient (at 20 °C between pH 5 and 7, data not shown) is consistent with a 1:1 electron/proton stoichiometry, allowing us to conclude that the two-electron hyper-reduction is coupled to the uptake of *two* protons. The overall process is complicated, and most importantly (see Discussion), it is a *slow* redox couple. The half-height width of the peaks at 20 mV s^{-1} yields an n_{app} value of approximately 1.04 (see eq 3), which suggests poor *cooperativity* between the two one-electron transfers, although inherently slow ET and slow proton transfer would also cause broadening, as would inhomogeneity of the enzyme film on the surface. The peaks sharpen with decreasing pH (although film instability precluded measurements below pH 5), suggesting that proton transfer is the rate-limiting reaction in reduction of $[3Fe-4S]^0$.

(39) The reduction potential varies slightly with buffer concentration; see Materials and Methods.

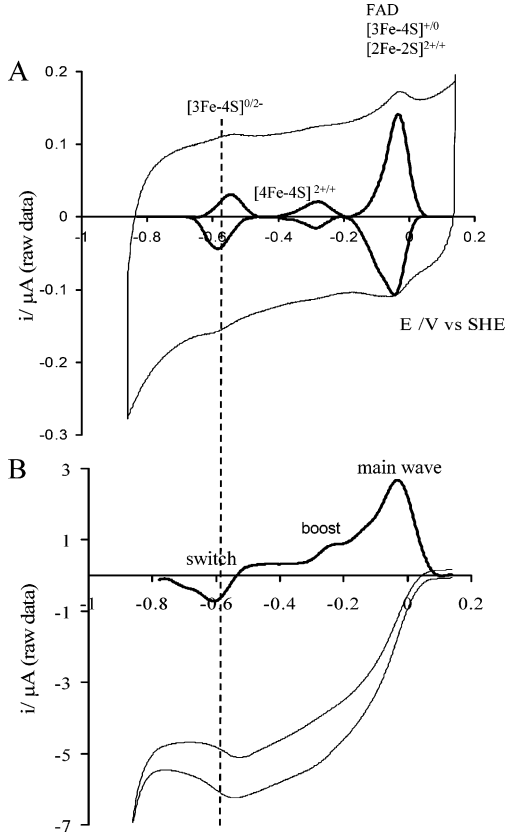

Figure 10. Hyper-reduction of the [3Fe−4S] cluster in WT FrdAB. (A) Noncatalytic data: raw (thin line) and baseline-subtracted (thick line). Note the additional peak at low potential that is not evident for pH > 7. Conditions: pH 5, 25 °C, scan rate = 20 mV s^{-1}. (B) Catalytic data showing a switch-off in activity at low potential (thin line) and the first derivative (thick line, Fourier-filtered) of the reductive scan. The vertical dashed line denotes the average reduction potential of the hyper-reduced [3Fe−4S] cluster, which corresponds closely with the switch potential. Conditions: pH 5, 25 °C, 5 mM fumarate, electrode rotation rate of 2000 rpm, and a scan rate of 20 mV s^{-1}.

Hyper-reduction of the [3Fe−4S] cluster leads to a drop in catalytic rate. As shown for WT in Figure 10B, taking the potential below −500 mV produces a marked attenuation which is reversible and becomes more prominent at lower pH, accounting for up to 40% loss of activity at pH 4.5. Comparison of catalytic and noncatalytic voltammograms obtained between pH 4.5 and 7 shows that the potential at which catalysis is attenuated correlates closely with the potential of the [3Fe−4S]$^{0/2-}$ redox couple (data shown for pH 5 in Figure 10A,B). Above pH 7, neither the attenuation of catalytic activity nor the redox transition of [3Fe−4S]$^{0/2-}$ is observed (H^+ is required in the reaction), whereas below pH 4.5, the voltammetry is too unstable to record. The sharp decrease in current below −800 mV is due to solvent breakdown (note that at pH 5, solvent breakdown occurs at a more positive potential than for pH 7 and is also evident for an electrode with no protein adsorbed). Although Y155S and L153C/Y155S both exhibited attenuation of activity at the same potential as WT, the effect was difficult to detect clearly for L153C.

Discussion

Evidence that the [3Fe−4S] Cluster is the Entry/Exit Point for Electrons. We consider first the question of how the enzyme is oriented at the electrode, and we assume that the structure of the membrane-extrinsic subcomplex FrdAB that we have studied is essentially the same as revealed in the crystal structure of the intact complex FrdABCD.[14] The crucial evidence we now consider is the effect of disabling the [3Fe−4S] cluster by forcing it into an inactive oxidation level.

Scheme 1. Coupled Protonation and Electron Transfers of the [3Fe−4S] Cluster

$$[3Fe\text{-}4S]^{+} \overset{1e^-}{\rightleftharpoons} [3Fe\text{-}4S]^{0} \overset{2e^-,\,2H^+}{\rightleftharpoons} [3Fe\text{-}4S]^{2-}\text{-}2H^{+}$$

Hyper-reduction of the [3Fe−4S] cluster and the attenuation of catalytic activity below −0.6 V are clearly related (Figure 10). Both properties only become visible below pH 7, and their potentials share the same pH dependence. At first glance, the attenuation in catalytic rate is contrary to what should occur were the potential of the center to be a key factor, since, as shown in Figure 2, there is now an excellent progression of driving force down the relay. The role of pH is possibly 2-fold. First, as established from other studies, further reduction of the [3Fe−4S]^0 cluster is totally dependent upon protonation.[16−19] The nature of the hyper-reduction reaction itself is not clear in this study since the peaks are broader than those observed in other proteins,[18] and it is possible (even likely) that two one-electron steps are involved, each requiring proton transfer. Whatever the exact details, the crucial point is that for FrdAB, cycling in the lower oxidation levels of the [3Fe−4S] cluster is slow and coupled to (and probably controlled by) obligatory proton transfer (Scheme 1).[40] Second, the normal turnover rate of fumarate reductase increases with decreasing pH (9−5), so that any effect on the catalytic current due to sluggish ET would become more apparent.

The [3Fe−4S] cluster therefore behaves as a "switch" at very low potentials, and the lower the pH, the more enzyme molecules are inactivated. Although the hyper-reduced [3Fe−4S] cluster is unlikely to have any physiological role, its generation at the electrode is informative. From the crystal structure, the [3Fe−4S] cluster lies at the end of the relay system and is the only obvious entry point for electrons to flow from the electrode into the enzyme (other entry points will involve much larger distances for intramolecular ET). The consequence of taking the potential down to very low values is to trap the [3Fe−4S] cluster in a lower, protonated oxidation level; this prevents it cycling between the + and 0 levels, thus curtailing its normal function and blocking the ET relay chain. Were electrons to enter at any other site in the relay, it is unlikely that hyper-reduction of the [3Fe−4S] cluster would make any difference to the catalytic activity (the [3Fe−4S] cluster is approximately 30 Å from the FAD). The inherent sluggishness of the hyper-reduction couple suggests also that its effect on catalysis is not due to the driving force for ET to the [4Fe−4S] cluster (approximately 0.3 V) falling in the Marcus inverted region. We conclude that the [3Fe−4S] cluster is an essential component of the electron transfer relay in FrdAB, and that in order to achieve the high catalytic rates that are observed, the enzyme must be oriented in the manner depicted in Figure 1.

Interpretation of the Reduction Potentials of the [4Fe−4S] Cluster. Reduction potentials of Fe−S clusters are controlled by several factors, including the distance and orientation

(40) Note that the [3Fe−4S] cluster may be performing an unusual fast, two-electron/two-proton transfer, as has been noted in studies on ferredoxins.[19] However, this process is unlikely to be useful in a one-electron relay.

of nearby dipoles or charged residues in the protein, the degree of solvent exposure, and the presence of hydrogen bonding.[41] A leucine side chain is incapable of hydrogen bonding, but a hydrogen bond could be formed between a free cysteine sulfur (as introduced in the FrdB mutant L153C) and a sulfur atom from the cluster or coordinating cysteine. The additional hydrogen bonding would stabilize the reduced cluster and, thus, raise the potential. In fact, the structure of *E. coli* SQR shows a hydrogen bond between Cys154 in the B subunit (equivalent to Leu153 in *E. coli* FrdB) and the thiol group of the ligating cysteine.[2] Shifting our focus to FrdB Tyr155, the crystal structure of the *E. coli* Frd has a resolution of 3.3 Å,[14] thus it is inconclusive on the presence of a hydrogen bond between Tyr155 and Cys154. However, replacement of Tyr155 with a serine (as in the mutant Y155S) could lead to weakened hydrogen bonding and a corresponding decrease in reduction potential. The effect on the reduction potential of the double mutant L153C/Y155S is the sum of the two individual mutations. Work by Denke et al. has shown similar relationships between hydrogen bonding and reduction potential in a Rieske center.[42] Although the reduction potential of the [4Fe−4S] cluster of *E. coli* SQR is reported to be 100 mV greater than that for *E. coli* Frd,[21] L153C/Y155S, the species that most closely mimics the sequence of *E. coli* SQR, has a reduction potential very similar to that of WT Frd.

Evidence That the Rate At Which the FAD Can Be Redox-Cycled Reversibly (at potentials close to its reduction potential) Does Not Depend on the Reduction Potential of the [4Fe−4S] Cluster. Earlier studies suggested that, due to its low potential, the [4Fe−4S] cluster in Frd need not be involved in ET to the flavin[43] or at least formed a secondary ET pathway.[13,44] However, the crystal structure of the intact complex FrdABCD has since shown that this *cannot* be the case. The [3Fe−4S], [4Fe−4S], and [2Fe−2S] clusters form a line from the quinone binding site to the FAD, and the [2Fe−2S] cluster (closest to the FAD) and the flavin are deeply buried (Figure 1).[14] As discussed above, disabling the $[3Fe-4S]^{+/0}$ redox couple shuts down catalysis, showing that the [3Fe−4S] cluster is essential and marking this center as the entry point in FrdAB. The distance between [3Fe−4S] and [2Fe−2S] clusters (20.3 Å) is too long to allow direct ET. Therefore, for electrons to reach the buried FAD, they must travel via the [4Fe−4S] cluster, which despite its low potential, *cannot* be bypassed. Discussion of intramolecular ET in FrdAB will first focus on explanations of the shape of the WT trumpet plots (in the absence, then presence of substrate), before turning to results for the mutants.

From pH 5−9, reduction of the FAD is accompanied by a single protonation, as shown by the −24 mV/pH unit dependence of reduction potential (average of oxidation and reduction peak potentials) at slow scan rates. Up to ∼10 V s^{-1}, there is little change in reduction potential, showing that transfer of two electrons and one proton are both complete on this time scale (0.2 s). Above this scan rate, the data shift *down* at pH 7 and *up* at pH 8.5, causing the plots to converge (Figure 5A). Crucially, the same peak positions were obtained whether starting from an oxidative or reductive poise.

We now consider explanations for the convergence of the peaks at high scan rates and recall that at a scan rate of 100 V s^{-1}, we are measuring ET energetics on the submillisecond time scale. First, it is possible that at high scan rates the FAD signal is no longer visible and the peak position is dominated instead by the high potential relay centers. This would imply that there is a problem with ET to the FAD; however, the [2Fe−2S] and [3Fe−4S] clusters are quite well separated in potential and have a small pH dependence (the equilibrium potentials of the [2Fe−2S] and [3Fe−4S] clusters shift −18 and −26 mV, respectively, from pH 7 to 8.5). Thus, were they to dominate the peak, it would be broad and unlikely to have the same potential over 1.5 pH units. Similarly, the peak cannot only represent the [3Fe−4S] cluster (closest to the electrode) since it is always significantly larger than the one-electron [4Fe−4S] peak. We, therefore, propose two alternative explanations, based upon the pH dependence of FAD reduction potential which shows that the overall two-electron reaction is coupled to the transfer of one proton. First, above a scan rate of about 10 V s^{-1}, the FAD may not have sufficient time to accept or donate a proton from/to the bulk solvent, but it is protonated instead by transfer from an internal group, making the bulk pH irrelevant at high scan rates. Indeed, the reduction potential that the trumpet plots converge to at high scan rates corresponds to that expected at pH 8.1 ± 0.3, quite close to the catalytic pK_a of 7.8 (data not shown), and thought to be due to the nearby His355.[45] The more likely option is that although the two-electron reduction of FAD is *cooperative* (n_{app} = 1.8, see Results), it is certain that the reaction actually proceeds via two one-electron reactions that are separated on a short time scale and must be punctuated by a proton transfer to compensate the charge (Scheme 2).

Scheme 2. Redox States of FAD

$$\mathrm{FAD} \underset{E_1}{\overset{1e^-}{\rightleftharpoons}} \mathrm{FAD^{\bullet -}} \overset{H^+}{\rightleftharpoons} \mathrm{FADH^{\bullet}} \underset{E_2}{\overset{1e^-}{\rightleftharpoons}} \mathrm{FADH^-}$$

Thus, commencing the cycle from an oxidative poise, FAD is reduced by a one-electron reaction to produce $FAD^{\bullet -}$, but the second electron does not follow until a proton is added to form $FADH^{\bullet}$. If proton transfer is slow relative to the scan rate, the peak will tend toward the potential value for the first ET with the remaining current due to proton-gated electron transfer appearing only as a "tail". In the limiting case, only a one-electron FAD peak would be observed at E_1. On the return scan, the oxidation comprises a one-electron reaction of $FADH^-$ to $FADH^{\bullet}$, followed by loss of a proton (forming $FAD^{\bullet -}$) and a second electron (resulting in FAD). In the limiting case, this produces a one-electron peak at E_2. Thus, at high scan rates, the FAD peak potentials deviate from E_{tot} (the two-electron, one-proton potential) toward the values appropriate to the first pure ET in each direction, resulting in pH-independent peaks. Due to the two-electron cooperativity, the second electron is more easily added than the first, so $E_2 > E_{tot} > E_1$; thus, at high scan rates, the oxidation peak is shifted higher toward E_2, while the reduction peaks are shifted lower toward E_1. In this

(41) Chen, K.; Bonagura, C. A.; Tilley, G. J.; McEvoy, J. P.; Jung, Y.-S.; Armstrong, F. A.; Stout, C. D.; Burgess, B. K. *Nat. Struct. Biol.* **2002**, *9*, 188−192.
(42) Denke, E.; Merbitz-Zahradnik, T.; Hatzfeld, O. M.; Snyder, C. H.; Link, T. A.; Trumpower, B. L. *J. Biol. Chem.* **1998**, *273*, 9085−9093.
(43) Manodori, A.; Cecchini, G.; Schroder, I.; Gunsalus, R. P.; Werth, M. T.; Johnson, M. K. *Biochemistry* **1992**, *31*, 2703−2712.
(44) Cammack, R.; Crowe, B. A.; Cook, N. D. *Biochem. Soc. Trans.* **1986**, *14*, 1207−1208.
(45) Pankhurst, K. L.; Mowat, C. G.; Miles, C. S.; Leys, D.; Walkinshaw, M. D.; Reid, G. A.; Chapman, S. K. *Biochemistry* **2002**, *41*, 8551−8556.

hypothesis, a larger peak separation results, which is dependent on the stability of the semiquinone. This produces a k_0' that underestimates the true rate of electron transfer to and from the FAD.

In a study of another fumarate reductase, flavocytochrome c_3 (Fcc$_3$) from *Shewanella frigidimarina*, we reported that the trumpet plot data (at high scan rates) in the presence of fumarate also lay *within* the data obtained without substrate.[33] We proposed that this arises because k_0' for the FAD is higher when fumarate is bound. Our new results now suggest an alternative explanation, namely, that fumarate binding causes a small stabilization of the semiquinone state. This would decrease E_2 and increase E_1, thus narrowing the trumpet plot and producing an apparently higher k_0'.

Whichever of these explanations hold, the fact that the trumpet plots for the FAD virtually overlay for each mutant shows that the ET rate is influenced very little by the [4Fe−4S] potential. Calculations based on an empirically derived equation[46] predict ET rates for the mutants that are 4.6, 0.3, and 1.3 times the WT rate for L153C, Y155S, and L153C/Y155S, respectively. Thus, the 100 mV difference between the [4Fe−4S] potentials of the L153C and Y155S mutants should (in the case of pure ET) have caused a 15-fold difference in ET rates, which is not observed.

Comments on Catalytic Rates Measured by Conventional Assays. Were there to be an advantage in smoothing out the potentials of relay centers in an enzyme in order to produce optimal catalytic rates, it would be expected that the L153C mutant, which has a thermodynamically less unfavorable reduction potential in the Fe−S cluster relay (Figure 2), would show an increased catalytic rate while Y155S should display a decreased rate. As with the rates of FAD redox cycling discussed above, the results do not support this hypothesis. It is important to note that the solution kinetics were performed using a large excess of reduced BV ($E^{0\prime} = -359$ mV[23]), likely to impose a potential well below the [4Fe−4S] potential for all mutants. However, we would expect that different results might be obtained if we used an electron donor with a reduction potential of the right value to engage the "boost" for some, but not all, of the mutants. In light of this work, we consider the results of Kowal et al. who studied the steady-state solution kinetics of the [4Fe−4S] cluster mutants C148S and C151S of the intact enzyme FrdABCD.[47] Replacement of cysteine by serine in these mutants lowered the reduction potential of the [4Fe−4S] cluster by 60 and 70 mV, respectively, compared to WT, making electron transport to the FAD thermodynamically less favorable. Fumarate reduction assays using BV showed only a slight difference in rates between the WT and the mutants (98 and 101% of WT), while assays using DMN (2,3-dimethyl-1,4-naphthoquinone), a much higher potential donor and analogue of menaquinone,[48] gave significantly lower rates for the mutants (57 and 23% of WT). These results can now be interpreted in terms of the steady-state catalytic rate of WT being boosted when the [4Fe−4S] cluster is maintained in the reduced state, whereas the [4Fe−4S] cluster in the mutants (which have more negative potentials) would be maintained at a more oxidized level.

The relatively poor control over thermodynamic driving force in the solution experiment highlights the advantage of the PFV technique, which reveals the potential dependence of catalysis. However, a disadvantage of PFV is that it is difficult to determine reliable catalytic kinetic parameters. Not only is it necessary to determine values for electroactive coverage by integration of nonturnover signals, but also the procedure involves extrapolation of current data to correct for the rotation rate dependence. Our efforts were therefore limited, the important point being to confirm that the maximum turnover rate for ET FrdAB at the electrode is 330 s^{-1}, which is fully consistent with the solution data.

Interpretation of the Effect of [4Fe−4S] Oxidation Level on Catalytic Rate. Our results show that the boost in catalytic rate (contributing up to 50% of the activity at low potentials) for each mutant correlates very well with the reduction potential of the [4Fe−4S] cluster in that mutant. This relationship may not have physiological relevance, as it is unlikely that the quinone pool that supplies electrons for fumarate reduction will ever impose a potential this low (<-300 mV). However, the results are important in understanding the overall mechanism of catalytic electron transport. We consider three options, based upon (1) the effect of the [4Fe−4S] cluster on rate-determining ET kinetics, (2) long-range intramolecular communication between the cluster and active site, or (3) a thermodynamic advantage that is gained for a situation in which *two* electrons must be transferred to the FAD.

The first option is that the boost in activity reflects an increase in the ET rate to the active site when the [4Fe−4S] cluster is reduced. The evidence suggests that ET to the FAD (with an *exchange* rate constant of at least 800 s^{-1}) is easily sufficient to maintain the steady-state catalytic rate, although it is still possible that ET could limit catalysis under certain conditions,[20] such as lower pH (pH < 6) where the turnover rate is higher (see solution kinetics data in Table 3). The option invokes an enhancement in ET rate when the electrode potential is sufficiently negative to ensure that the [4Fe−4S] cluster is held mainly in its reduced state. This might arise in three ways. (a) An electrostatically induced alteration in conformation (slow compared to the ET rate) improves electron coupling. For example, the [4Fe−4S] cluster in its reduced state might move slightly closer to either of the other clusters. However, the difference in energies between any such conformations would have to be less than 20 meV based on the symmetry of the [4Fe−4S] cluster trumpet plot (Figure 5B). (b) ET occurs via a super-exchange mechanism, so that a reduced [4Fe−4S] cluster provides a better pathway. (c) *Direct* electron exchange between the electrode and the [4Fe−4S] cluster (which is located approximately 12 Å from the protein surface) provides another

(46) This equation (described in ref 7 and in: Page, C. C.; Moser, C. C.; Dutton, P. L. *Curr. Opin. Chem. Biol.* **2003**, *7*, 551−556) describes the ET rate constant within proteins in terms of the distance between centers, the packing density of the protein, the change in free energy, and the reorganization energy. The calculation included a standard value for the protein packing density as 0.75, reorganization energy of the Fe−S clusters as 0.7 eV, and the edge−edge distances from the WT crystal structure. The ET rate for each mutant was based on the step from the [3Fe−4S] to the [4Fe−4S] cluster since this is the most energetically unfavorable step and would most likely be rate-determining if energetics were to control the inherent kinetics of electron flow along the relay.

(47) Kowal, A. T.; Werth, M. T.; Manodori, A.; Cecchini, G.; Schroeder, I.; Gunsalus, R. P.; Johnson, M. K. *Biochemistry* **1995**, *34*, 12284−12293.

(48) Menaquinone is reported to have a reduction potential of −74 mV at pH 7 for the two-electron reaction (Wissenbach, U.; Kröger, G.; Unden, G. *Arch. Microbiol.* **1990**, 154, 60−66). For DMN (2,3-dimethyl-1,4-naphthoquinone), a reduction potential of −240 mV is reported for the one-electron reduction of quinone to radical (Ilan, Y. A.; Czapski, G.; Meisel, D. *Biochim. Biophys. Acta* **1976**, *430*, 209−224).

entry point for electrons. Thus, poorly oriented enzyme molecules or those with damaged/absent [3Fe−4S] clusters might contribute to activity. However, reiterating our earlier discussion about our evidence for the [3Fe−4S] cluster being the entry/exit point, we believe possibility (c) is unlikely. During extensive studies with different samples of FrdAB, including nonrecombinant enzyme, we have never observed catalytic voltammetry in which the boost became the most prominent feature.

The problem is that none of these explanations account for the enhanced rate of slow release of OAA concomitant with [4Fe−4S] cluster reduction, and we now discuss this result. The second option is that the oxidation level of the [4Fe−4S] cluster influences the events occurring at the active site or controls the entry and exit of substrates. An important clue as to what this entails stems from the experiments with OAA, the results of which demonstrate *unequivocally* that its rate of release from the active site depends on whether the [4Fe−4S] cluster is oxidized or reduced (shown both by the potentials involved and the fact that it is a one-electron, not a two-electron, process). The instrumental errors in these experiments are small, as the rates are easy to measure and the potential dependences are clearly defined. As well as being orders of magnitude slower than ET, the binding and release rates of OAA are much slower than those for fumarate and succinate. This may be because the enzyme active site requires OAA to tautomerize from the keto to the enol form (which more closely resembles fumarate) before it will bind. This process is likely to occur within the protein binding pocket rather than in solution since the binding and release of OAA in the related enzyme Fcc_3 from *S. frigidimarina* are rapid (data not shown).[49] Thus, the significant enhancements in OAA release upon reduction of the [4Fe−4S] cluster suggest that the boost in catalytic activity might be due to an increase in the rate of a process that causes release of the product or adjusts the position of the substrate. This would be consistent also with the boost only occurring at high turnover rate (at high substrate concentrations) since the product release rate becomes more significant.[50]

However, this mechanism must invoke a long-range interaction that is difficult to explain (the [4Fe−4S] cluster and the active site are approximately 20 Å apart). It is possible that because ET to the [4Fe−4S] cluster is not coupled to proton transfer, the reduced state $[4Fe-4S]^{+}$ buries an additional negative charge in the enzyme, providing a perturbation that is sufficient to alter the properties of the active site. The lower OAA release rate and seemingly smaller boost of L153C may also relate to this mutant's lower activity. For all of the mutants, the OAA release rate is enhanced; the fact that the L153C mutation creates a smaller effect may highlight further the subtlety of the long-range interaction that is required.

The third option for explaining the boost is that maintaining the [4Fe−4S] cluster in the reduced state facilitates the transfer of *two* electrons to the FAD, the point being that the FAD radical is inherently unstable. Drawing an analogy to a baseball game, this would be analogous to having a runner (electron) on both second ([4Fe−4S]) and third ([2Fe-2S]) bases, making it easier to get two runners home (FAD). The low potential of the [4Fe−4S] cluster "sharpens" the advantage that this site be permanently populated. This situation is illustrated in Figure 11. It is essentially a thermodynamic argument in that it assumes that electron transfer along the Fe−S relay is fast and reversible and should be regarded as a pre-equilibrium,[32] preparing the enzyme for the rate-determining reduction of fumarate at the FAD. This model is more generally consistent with the kinetic data, which show that the maximum turnover rates for the enzymes are significantly less than the electron exchange rates for both the FAD and the [4Fe−4S] clusters, noting further that exchange rates represent a lower limit in the absence of any driving force. Once the electrode potential is low enough to ensure there is an electron on the [4Fe−4S] cluster, the subsequent transfer of two electrons to the FAD becomes more favorable.

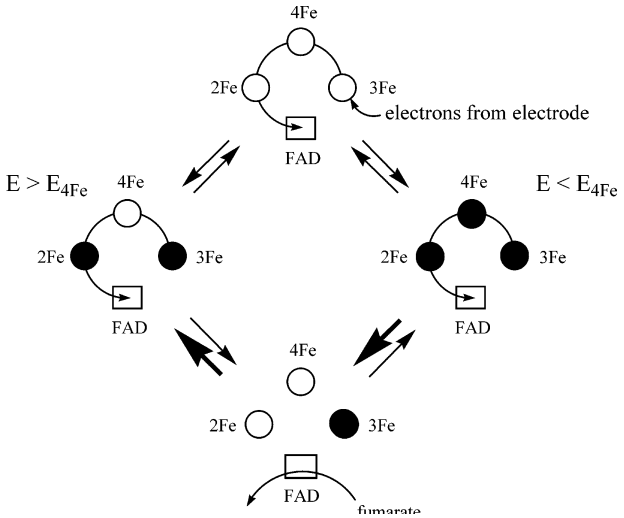

Figure 11. Cartoon illustration of the "baseball game" analogy for catalytic electron transport in fumarate reductase. Electrons move from the electrode "in an anticlockwise direction" via the [3Fe−4S], [4Fe−4S], and [2Fe−2S] cluster to the FAD. Black "bases" represent reduced cofactors, while empty "bases" represent oxidized cofactors. In the first stage, it is the applied electrode potential which determines whether two or three Fe−S clusters ("bases") are populated with electrons ("runners"), the [4Fe−4S] cluster being populated substantially only when the electrode potential is decreased below its reduction potential ($E < E_{4Fe}$). In the second stage, electrons are distributed within the enzyme to produce two-electron-reduced FAD, which is then ready to be regenerated by fumarate reduction. The second stage is an internal pre-equilibrium, with two-electron reduction of FAD being favored when the [4Fe−4S] cluster also has an electron (right).

This model can also explain the OAA release results since FAD reduction is a prerequisite for OAA release.[51] This "baseball game analogy" for ET in fumarate reductase is an interesting but complex possibility that cannot be discounted at this stage without further research and simulations. The model is fully consistent with the proposal made by Dutton and coworkers, which is that ET along intramolecular relays in enzymes has usually evolved to be fast enough so as not to be rate-determining in catalysis.[7] In our study, the thermodynamic characteristics of the relay are revealed because of a special combination of the two-electron preference of the FAD and the positioning of the low potential cluster two sites away.

(49) These OAA release rates were measured in the presence of chloride, which (like other anions) has been shown to bind to the active site. The presence of chloride in these experiments is responsible for the higher release rates and weaker binding reported here compared to those measured previously (see ref 13).

(50) Butt, J. N.; Thornton, J.; Richardson, D. J.; Dobbin, P. S. *Biophys. J.* **2000**, *78*, 1001−1009.

(51) It is known also that malate can be oxidized to OAA by SQR (ref 38), thus enhanced release of OAA by a very slow catalytic reduction process, which might somehow be enhanced by the delivery of two electrons, also remains a possibility. Although OAA reduction could not be detected with PFV, more sensitive gas chromatography analysis of the products after bulk catalysis may provide more evidence for this possibility.

Conclusions

The object of this study has been to study the functional requirements of a multicentered ET relay system, as occurs in numerous enzymes, but exemplified here by the crystallographically characterized fumarate reductase from *E. coli*, the water-soluble form of which displays excellent electron transfer and catalysis when adsorbed on an electrode. The evidence that the relay system is dependent upon the [3Fe−4S] cluster being able to operate in the normal +/0 redox couple marks this center as an essential ET site, and its crystallographically defined location places it at the start of the relay. Electrons must transfer next to the [4Fe−4S] cluster, and we have established that the rates of FAD redox cycling and catalysis are not significantly perturbed by a 100 mV change in reduction potential when the measurement is being made at a fixed, moderate potential. These results provide support for the proposal that reduction potentials of components of intramolecular electron relays do not need to be finely tuned by evolution because ET is usually fast compared to the true catalytic rate.[7] However, the rate of catalysis does depend on whether the reaction is being driven at a potential above or below the potential of the [4Fe−4S] cluster; in fact, maintaining the [4Fe−4S] cluster in the reduced state *boosts catalysis* by up to 50%. This is highly informative since the most likely explanation is that the relay operates in *a fast and reversible manner*. In this model (the baseball game analogy), supply of two electrons to the FAD is treated as a rapid pre-equilibrium, in which there is a thermodynamic advantage in having both proximal ([2Fe−2S]) and medial (4Fe−4S]) clusters "loaded" with an electron.

Acknowledgment. This work was supported by BBSRC Grants 43/10492, 15/C12775, and 43/B19096, and by NIH GM61606, and the Department of Veterans Affairs. J.M.H. wishes to thank the UK ORS Award Scheme, St. Edmund Hall and the University of Oxford Clarendon fund, and the University of Sydney Travelling Scholarship. We thank Drs. Christophe Léger, Christopher Blanford, Tina Iverson, and Laurent Fillisetti for helpful discussions.

Supporting Information Available: Deconvoluted noncatalytic voltammograms for WT and mutants (PDF). This material is available free of charge via the Internet at http://pubs.acs.org.

JA043404Q